

ELECTRONIC SUPPLEMENTARY INFORMATION

Synthetic procedures

The ligand was prepared as previously reported by us (Colacio et al. Inorg. Chem. 2011, 50, 7268).

Synthesis of 1.- To a solution of H₂L (56 mg, 0.125 mmol) in 5 mL de MeOH were added with continuous stirring 54.8 mg (0.125 mmol) of Dy(NO₃)₃·5H₂O. The resulting colourless solution was filtered and allowed to stand at room temperature. After one day, well formed prismatic colourless crystals of the compound were obtained with yield 65% based on Dy.

%Cexp = 37.53	%Ccalcd = 37.79
%Hexp = 5.73	%Calcd = 5.52
%Nexp = 9.95	%Calcd = 9.79

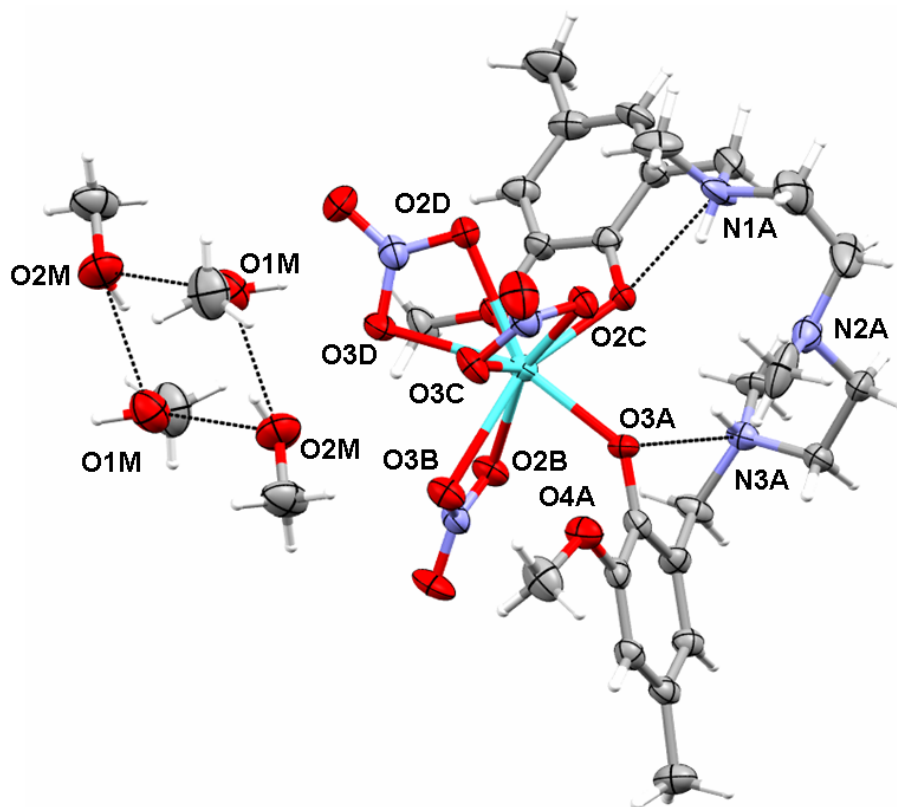


Figure S1.- Perspective view of the structure of **1** with hydrogen bonded methanol crystallization molecules. Thermal ellipsoids are shown at 50 % probability

Physical measurements

Elemental analyses were carried out at the “Centro de Instrumentación Científica” (University of Granada) on a Fisons-Carlo Erba analyser model EA 1108. IR spectra on powdered samples were recorded with a ThermoNicolet IR200FTIR using KBr pellets. Magnetisation and variable temperature (2-300 K) magnetic susceptibility measurements on pellets of polycrystalline samples were carried out with a Quantum Design SQUID MPMS XL-5 device operating at different magnetic fields. The experimental susceptibilities were corrected for the diamagnetism of the constituent atoms using Pascal’s tables.

Crystallographic data and Refinement

X-ray crystal data for **1** were collected with a Bruker AXS APEX CCD area detector equipped with graphite monochromated Mo K α radiation ($\lambda = 0.71073 \text{ \AA}$) by applying the ω -scan method. Lorentz-polarization and empirical absorption corrections were applied. The structures were solved by direct methods and refined with full-matrix least-squares calculations on F^2 using the program SHELXS97¹. Anisotropic temperature factors were assigned to all atoms except for the hydrogens, which are riding their parent atoms with an isotropic temperature factor arbitrarily chosen as 1.2 times that of the respective parent. Final $R(F)$, $wR(F^2)$ and goodness of fit agreement factors, details on the data collection and analysis can be found in Tables S1.

(1) G. M. Sheldrick, *Acta Crystallogr. Sect A*, **2008**, 64112.

Table S1.- Crystallographic data for **1** and **1'**.

Complex	1	1'
Formula	C ₂₇ H ₄₇ N ₆ O ₁₅ Dy	C ₂₇ H ₄₇ N ₆ O ₁₅ Dy _{0.11} Y _{0.89}
M _r	858.21	792.71
Crystal system	Triclinic	Triclinic
Space group (no.)	P-1 (2)	P-1 (2)
a (Å)	9.7795(10)	9.7740(18)
b (Å)	12.3752(13)	12.368(2)
c (Å)	15.1260(16)	15.119(3)
α (°)	76.3780(10)	76.302(3)
β (°)	86.1800(10)	86.088(3)

γ (°)	81.4960(10)	81.445(3)
V (Å ³)	1758.6(3)	1754.9(6)
Z	2	2
D_c (g cm ⁻³)	1.621	1.5
$\mu(\text{MoK}_\alpha)$ (mm ⁻¹)	2.200	1.789
T (K)	100(2)	100(2)
Observed reflections	6175 (5368)	6161 (5281)
R_{int}	0.0485	0.0426
Parameters	451	451
GOF	1.028	1.028
R_1^a	0.0464 (0.0380) ^b	0.0559 (0.0462) ^b
wR_2^c	0.0861 (0.0817)	0.01188 (0.1121)
Largest difference in peak and hole (e Å ⁻³)	1.212 and -0.535	1.237 and -0.413

^a $R_1 = \sum |F_o| - |F_c| / \sum |F_o|$.

^b Values in parentheses for reflections with $I > 2\sigma(I)$.

^c $wR_2 = \{\sum [w(F_o^2 - F_c^2)^2] / \sum [w(F_o^2)^2]\}^{1/2}$

Computational details

All calculation have been performed with the MOLCAS 7.2 package.¹ MOLCAS ANO-RCC basis set has been used for all the atoms, with the exception of Dy^{III} which has been treated with an embedding model potentials (AIMP).² The following contractions were used: Dy [9s8p6d4f3g2h]; Co [6s5p4d2f]; O [4s3p1d]; N [4s3p1d]; C [3s2p] and H [2s].

To compute the g axis for the Dy^{III} cation a complete active space self-consisting field (CASSCF) calculation has been performed with an (9,7) active space and 21 sextets, 128 quadruplets and 130 doublets have been mixed into the restricted active space state interaction (RASSI-SO) procedure. Finally, the g axis values were extracted form MOLCAS output (CASSCF/RASSI calculations) by using the SINGLE_ANISO computer code.³

- [1] M. Casarrubios, L. Seijo, *J. Chem. Phys.* **1999**, 110, 784.
- [2] G. Karlstrom, R. Lindh, P. A. Malmqvist, B. O. Roos, U. Ryde, V. Veryazov, P. O. Widmark, M. Cossi, B. Schimmelpfennig, P. Neogrady, L. Seijo, *Comput. Mater. Sci.* **2003**, 28, 222 – 239.
- [3] a) L. F. Chibotaru, L. Ungur, C. Aronica, H. Elmoll, G. Pilet, D. Luneau, *J. Am. Chem. Soc.* 130 (2008), 12445. L. Ungur, W. Van den Heuvel, L. F. Chibotaru, *New J. Chem.* 33, (2009), 1224.

Measurements on aligned microcrystals

A mixture of the powdered microcrystalline sample of **1** and eicosane was heated at 320 K and then a *dc* field was applied up to 5 T. At this field the principal axis of the microcrystals should be largely aligned along the magnetic field. After cooling at 2 K, the magnetization became almost saturated at 2 T with a saturation value of $8.5 \text{ N}\mu_{\text{B}}$, thus indicating the presence of strong axial anisotropy (Figure S2). The expected saturation value for a Dy^{3+} ion with easy-axis anisotropy and a $J_z = \pm 15/2$ ground Kramers doublet of $10 \text{ N}\mu_{\text{B}}$ is not reached probably because of the deviation of crystals from the complete alignment.

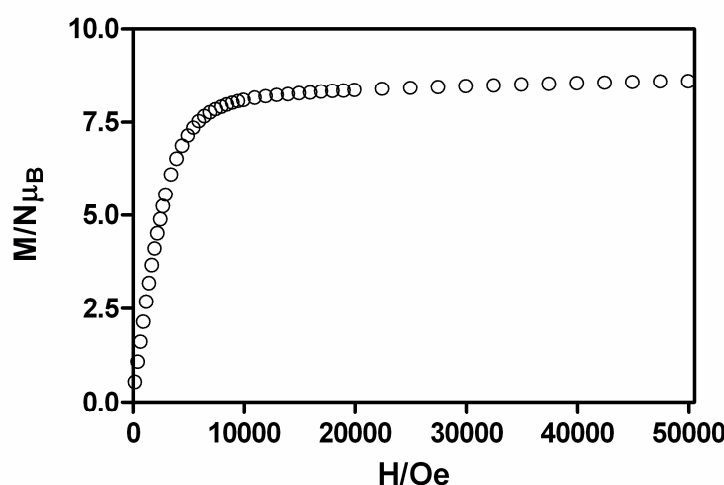


Figure S2. M vs. H plot for **1** at 2 K in eicosane after heating the sample under an applied field of 5 T at 320 K.

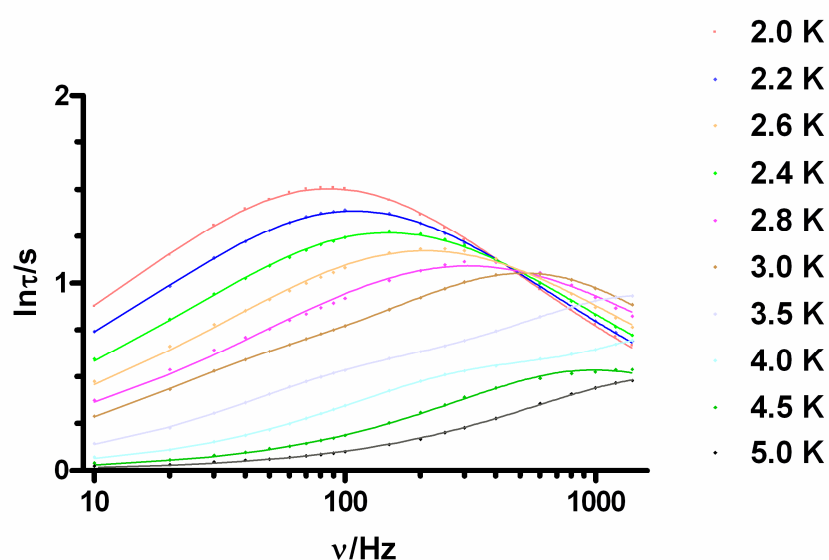


Figure S3. Frequency dependence of the *ac* out-of-phase susceptibility for **1** at different temperatures. Solid lines show the best fit to the sum of two modified Debye functions.

Table S2.- Relaxation times and α values for **1**.

	FR		SR	
	τ	α	τ	α
2.0 K	0.001844	0.366		
2.2 K	0.001467	0.370		
2.4 K	0.001072	0.3710		
2.6 K	0.000758	0.3718		
2.8 K	0.000515	0.3878		
3.0 K			0.04091	0.1336
3.5 K			0.000116	0.1451
4.0 K			0.000403	0.1751
4.5 K			0.000149	0.1801
5.0 K			0.0000769	0.1861

Table S2.- Relaxation times and α values for **1'**.

	FR		SR	
	τ	α	τ	α
2.0 K	0.00830	0.289		
2.2 K	0.00550	0.274		
2.4 K	0.00329	0.273		
2.6 K	0.00187	0.269		
2.8 K	0.00092	0.249		
3.0 K			0.0079	0.0401
3.5 K			0.00259	0.0448
4.0 K			0.00089	0.0506
4.5 K			0.00026	0.1011
5.0 K			0.00011	0.1238

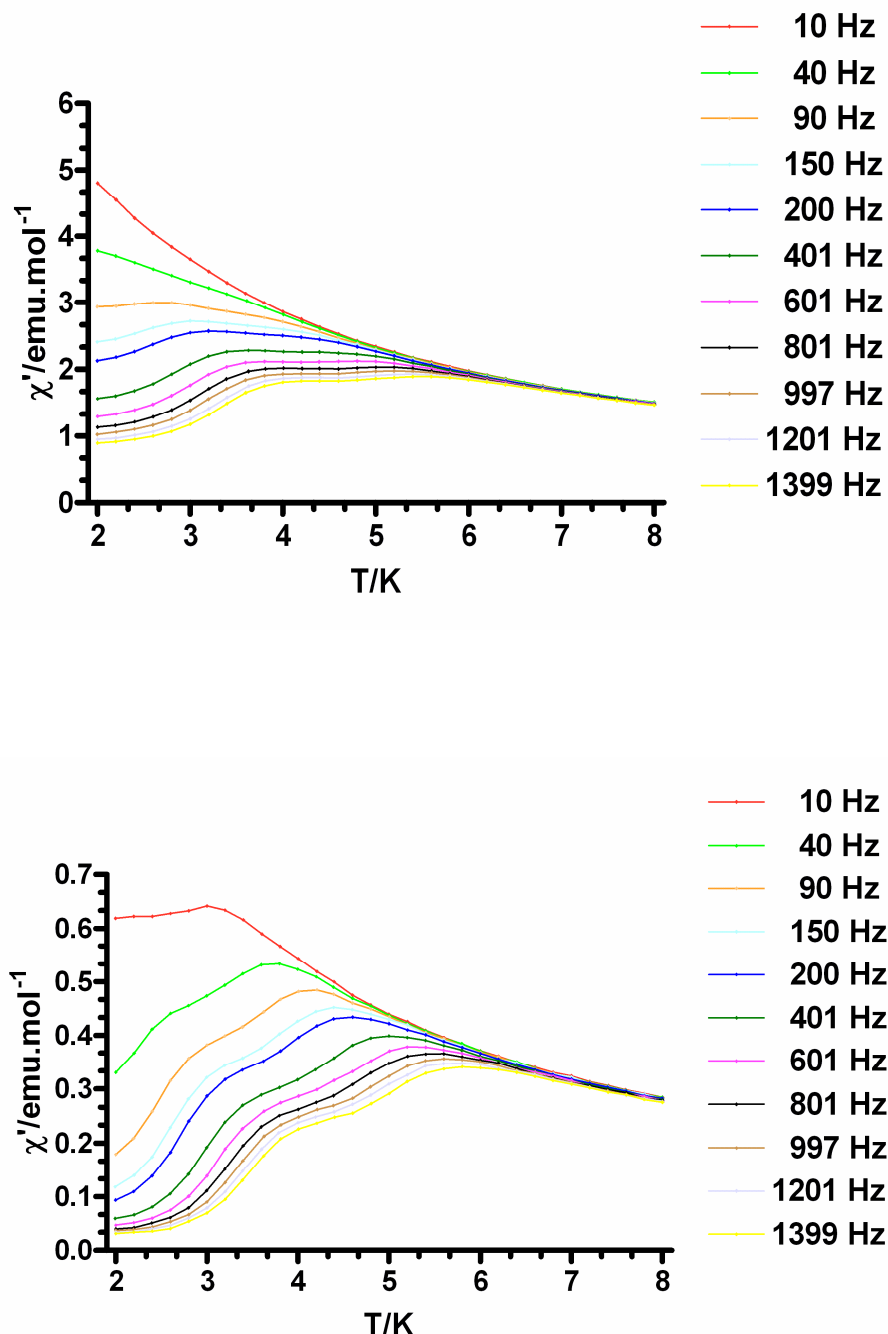


Figure S4 Temperature dependence of the in-phase ac susceptibility for **1** (top) and **1'** (bottom) at different frequencies.

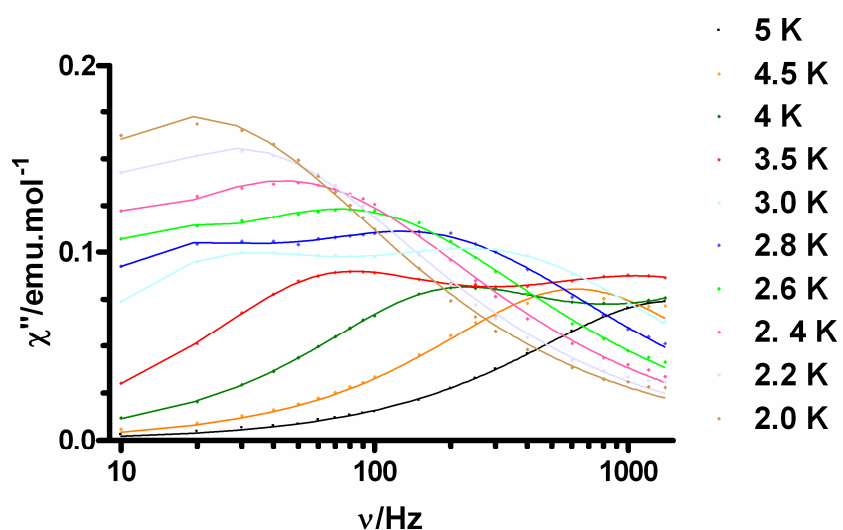


Figure S5.- Frequency dependence of the out-of-phase ac susceptibility for **1'** at different temperatures. Solid lines show the best fit to the sum of two modified Debye functions.

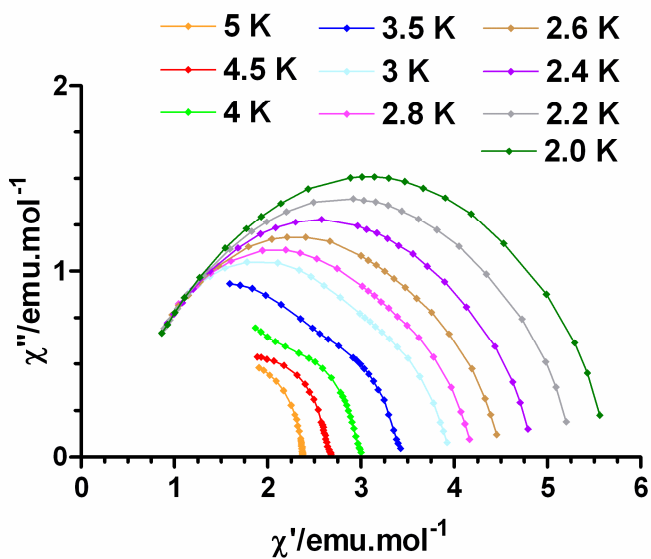


Figure S6.- Cole-Cole plot for **1**

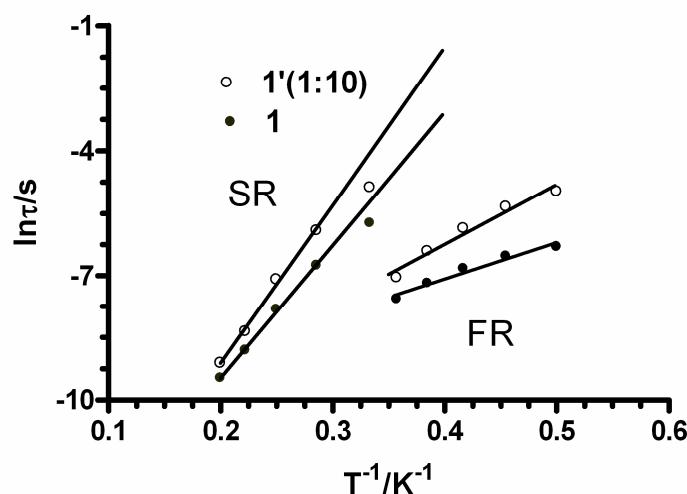


Figure S7. Arrhenius plot for **1** and **1'**.

It should be underlined that we have measured several fresh crystalline samples coming from different preparations and in all cases two out-of-phase peaks were observed. Moreover, the powder X-ray diffractogram matches well with the theoretical one (figure S8) and therefore the presence of a magnetic impurity responsible of the FR peak can be ruled out.

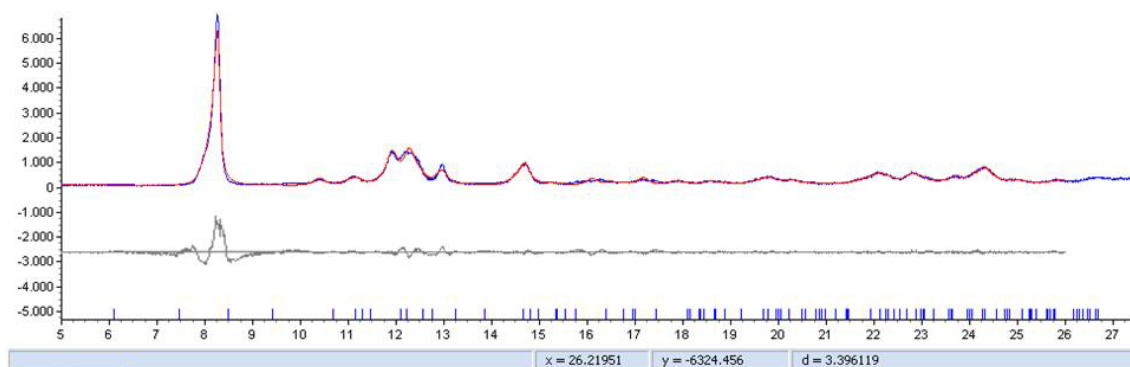


Figure S8: LeBail refinement of **1**. Experimental (red), calculated (blue) and difference (grey).